

Microsimulation Calibration Using Speed Flow Relationships

Authors

Sandeep Menneni and Carlos Sun, Ph.D., P.E.
Civil and Environmental Engineering
University of Missouri-Columbia
E2509 Lafferre Hall, Columbia, Missouri 65211, U.S.A.
Email: csun@missouri.edu, Telephone: 573-884-6330, Fax: 573-882-4784

Peter Vortisch
PTV AG,
Stumpfstr. 1, D-76131 Karlsruhe, Germany
Email peter.vortisch@ptv.de, Telephone ++49/721/9651/305

Document Length

Text (Excluding Tables and Figures) = 5343
Figures and Tables = $8 \times 250 = 2000$
Total = 7343

Submission Date: July 31, 2007

ABSTRACT

A microsimulation calibration methodology based on matching speed-flow graphs from field and simulation is presented. Evaluation and automation of matching speed-flow graphs is based on methods from pattern recognition. The methodology has been applied to US101 freeway network in San Francisco, California using an Evolutionary Algorithm. The methodology is compared to traditional methods of calibration based on capacity and is shown to perform better. In addition, a small scale test network simulation model was developed to assist in implementation of this methodology for large simulation models. The performance of the test network simulation model is comparable to the US101 simulation model.

INTRODUCTION, LITERATURE REVIEW AND MOTIVATION

Various methodologies have been proposed for calibration of microsimulation models. Dowling et al. (1) propose the use of three-step methodology: capacity calibration, route choice calibration, and system performance calibration. Hourdakis et al. (2) propose the use of three stage calibration: volume-based calibration, speed-based calibration, and an optional objective-based calibration. Dowling et al. (1) also propose that calibration of the model to capacity be one of the first steps in microsimulation calibration. It is also suggested that queue discharge flow rate be used to estimate a numerical value for capacity. Most of the objective functions for measuring the difference between field and measured discharge flows are based on different statistical goodness-of-fit measures (Dowling et al. (1), Toledo et al. (3), Schultz et al. (4)). Gomes et al. (5) describes a unique calibration methodology of matching the location of bottlenecks, queue lengths, and HOV lane utilization.

One motivation for this paper stems from concepts of capacity. The Highway Capacity Manual's (HCM) capacity definitions and its various clarifications ((6), pg. 2-2, 13-2) could be interpreted in several ways, even though HCM clearly notes some of the important concepts underlying the definition of capacity like reasonable expectancy, reproducibility, and sustainability. All these concepts cannot be easily captured through a single numerical value of capacity. These concepts are important in order to implement the capacity calibration process in the calibration procedure. Capacity is an important parameter that defines a facility and its operational capability. However, defining capacity as a single numerical value results in loss of information. A distribution of capacity values has more information than a single numerical value. There have been recent studies which address the stochastic nature of capacity (Brilon et al. (7)). If capacity calibration process is based on a single numerical value, matching the means of capacity distribution does not necessarily match the other important properties of a distribution; for example, spread, shape, and median. This concept can be extended further to include other traffic parameters like speed. For instance, is it important to match speed at which capacity values are observed? There are many studies that demonstrate that there are two different types of maximum flows observed in the field, one is queue discharge flow (QDF) and the other is pre-queue flow (PQF) (Banks (8)). Each of these flows is sustained for a different amount of time. With-respect-to calibration, is QDF or PQF more important to be matched? The authors suggest the matching of both values. In summary, it is important to maximize the information used during the calibration process.

The other motivation for this paper stems from the need for developing the optimization process for calibration. Due to the stochastic nature and complexity of microsimulation model, representation of microsimulation as closed-form equation is not usually possible. As a result, traditional calculus based optimization methods cannot be applied (1). The calibration of simulation models requires the use of other search and optimization methods based on multiple evaluations of the objective function. There are many such methods that can be applied to microsimulation calibration. Most of these methods direct the search path based on multiple evaluations of the objective function. The amount of information available in an objective function is of utmost importance; therefore, speed-flow graphs could perform better since they contain more information. For example, if minimization of the difference of numerical capacity values is the objective, there always exists a possibility of optimization method recommending non-optimal parameters, because the degree of freedom is too high. A possible solution is to expose only the calibration parameters that have a significant effect on the objective function. However, by using speed-flow graphs, a higher number of parameters can be exposed to the calibration process, resulting in a better fine-tuned simulation model. In case of single numerical values, different statistical goodness-of-fit measures are available. But how does one measure the closeness of two graphs or two point sets? Statistical formulation of goodness-of-fit measures is usually not possible without parameterization of the point sets. A similar problem has been studied in the field of pattern recognition. The statistical goodness-of-fit measures are similar in nature to measures of similarity or dissimilarity in pattern recognition. A modified pattern recognition method capable of being used as a fitness measure is presented in the objective function section.

METHODOLOGY

Speed-Flow Graphs

Speed-flow graphs have been used to describe operational capabilities of highways, and in developing macroscopic relationships for freeways. It is relatively easy to collect speed, flow, and occupancy information due to wide use of instrumentation on freeways. Speed-flow graphs contain much information as described below. It is the intent of this calibration methodology to use such information available in speed-flow graphs. This methodology is based on matching speed-flow graphs obtained from simulation and field. The HCM (6) divides speed-flow graphs into three regions: free-flow, congested, and queue discharge. The HCM concepts of capacity are well represented through speed-flow graphs. As a result, capacity information is available in a speed-flow graph. QDF and PQF information can also be derived from speed-flow graphs. In addition, speed-flow graphs also provide information about free-flow and congested regions, which is not present in a single numerical value or distribution of capacities. A calibration procedure based on speed-flow graphs, which provides information about all the three regions: free-flow, congested, and queue discharge could replicate the whole range of traffic behavior and not just peak period. One could also just use a portion of the speed-flow graph instead of the entire graph for calibration such as the queue discharge region. It is important to recognize that speed-flow graphs lack information about time. However, intensity of points in speed-flow graphs contains partial frequency information. Hence, the concept of sustainability is only partially captured in a speed-flow graph. An alternate graph, maximum flow sustained time graph, based on the concept of maximum flow sustained over different periods of time provides a better picture of the flow sustainability concept in capacity definition. However, due to the stochastic nature of both real and simulated traffic flows, it would not be possible to exactly replicate a volume-over-time curve. Despite the fact that fluctuations and breakdowns will not occur at exactly the same time in the real-world as in simulation, the simulation model is nevertheless correctly calibrated.

The concept of replicating field speed-flow graphs has been used in a number of previous studies. Wiedemann (9, 10) used speed-flow graphs to demonstrate closeness of field and simulation model. Fellendorf and Vortisch (11) demonstrated the ability of a simulation model to replicate speed-flow graphs from real-world freeways. However, it is hard to find literature which has used speed-flow graphs in the microsimulation calibration process. Ngoduy et al. (12) used an objective function based on speed and flow, which is mathematically close to replicating speed-flow graphs, for calibration of a macroscopic simulation model. The calibration of speed-flow graphs is just one step in microsimulation calibration and should be followed by route-choice calibration and system performance calibration.

In developing a speed-flow graph, the importance of location for collecting speed-flow graphs has been demonstrated by May (13). Data can be collected over different locations and multiple days and combined to show a complete speed-flow graph. In terms of field data, speed and flow information for the section under consideration can be collected for instrumented highways over many locations and different days. The simulation data can be collected by placing detectors at exactly the same locations as detectors in the field.

Pattern Recognition Based Objective Function

The objective function used in calibration is based on the concept of reducing the difference between speed-flow graphs obtained from field and simulation. For comparing speed-flow graphs researchers have tested the closeness of the graphs by visually matching the simulated and field graphs. A fitness function for measuring closeness of simulated and field speed-flow graphs is needed. In addition, the fitness function should be automated and consistent across multiple evaluations. The development of an automated comparison method to replace manual eyeballing has the following benefits:

1. Multiple simulation runs can be compared without human intervention.
2. Maintains consistency across multiple comparisons.
3. Produces a quantitative value for the objective function.

The use of a mathematical formulation for testing the closeness of graphs has been used for many years in the field of pattern recognition for retrieving or matching images. The measures of closeness are often referred to in the field of pattern recognition as similarity measures. Alternately, the same problem can also be formulated using dissimilarity measures. A generic objective function based on minimizing the dissimilarity between speed-flow graphs was developed.

In order to formulate a fitness function to measure the dissimilarity of speed-flow graphs, a closer look at important properties like shape, scatter, extent, and intensity is necessary. Since the speed and flow measurements are stochastic in nature, it is also required to account for such a noise created in the speed-flow graphs. Dissimilarity measures are easily defined for points, but are harder for point sets. One of the more prominent dissimilarity measures for point sets is the Hausdorff distance (14). But, Hausdorff distance does not effectively represent shape created by the point sets and is not robust against outliers or noise (14). However, a different distance measure, which is based on template matching in pattern recognition, is more appropriate to the problem at hand. An important part of a speed-flow graph is its shape. Shape can be described in terms of area. The dissimilarity of two graphs can be measured by calculating the amount of area that is not covered by the other. Since speed and flow measurements are represented as point sets, discretization to convert point information to area is necessary. The discretization also has the effect of smoothing thus reducing noise in speed and flow measurements for matching purposes. Since the information coming from the field and simulation is often just partial and not a complete speed-flow graph, the comparison is only made over the space occupied by the field graph. The objective function, Z , for the calibration process of the field is as follows:

Min. Z = Sum of all the speed-flow area in the field data that is not covered by the simulated data.

Pseudo-code for fitness function evaluation

```
BEGIN
  CONVERT field and simulation vector data to raster data at a certain resolution
  FOR every cell in field data
    CHECK IF the same cell has a value in simulation data
      IF
        TRUE continue
        FALSE increment the objective function by a certain value
      END
  RETURN the final objective function value
END
```

This objective function does not capture the frequency of occurrence of speeds and flows. This information is purposely left out for reasons mentioned in an earlier section. The objective function is consistent over different evaluations, because the number of speed-flow points developed by the simulation model across each evaluation is constant. In order to compare the described methodology with existing methodologies two additional objective functions are used. These two objective functions are

1. Minimize the difference between maximum 5 min. flows observed in the field and simulation.
2. Minimize the difference between maximum 5 min. flow sustained over 15 min. observed in field and simulation.

There are ramifications related to the use of different aggregation period for speed and flow data. If speed and flow information is collected and aggregated over a five minute interval, the simulation model might need to be run for long periods of time and over many random seeds to develop a reasonable sample of points. For example, if data is aggregated over five minute intervals, it would require about 16 simulation-hours to produce 500 points on the speed-flow graph. The amount of time required to run 16 simulation-hours depends on the size of the microsimulation model. In addition, most of the optimization methods available are based on multiple evaluations of the microsimulation model.

Test Network

In order to keep the amount of time required to produce a reasonable number of sample points to a minimum, it might be advantageous to use a test network, instead of an actual network, to assist in optimization of calibration parameters by producing speed-flow graphs. Test network is a small-scale network developed to produce the widest range of speed and flows over the least amount of time (Figure 1). However, the use of test network for calibration is only valid under the assumption that speed-flow graphs from a test network are equivalent to the graphs produced by an actual network. Test network also provides other advantageous in calibration process. A simple test network was developed to replicate different flow conditions and a complete speed-flow graph. It is important to produce different range of operations to develop complete speed-flow graphs.

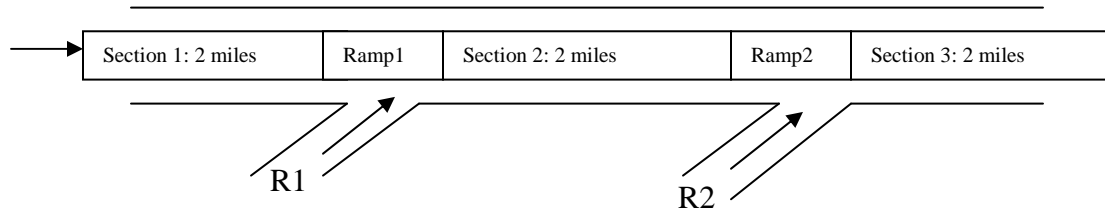


FIGURE 1 Illustration of the test network.

Figure 1 shows an example of a test network that consists of a mainline and two ramps. The mainline is approximately 6 miles long, and two ramps are placed at 2 miles apart. The mainline has the same number of lanes as the actual network. Detectors are placed every $\frac{1}{4}$ mile and no detectors are placed near the influence area of on-ramps to avoid distorted results. A total of 9 detectors (3 in each section) are placed on the mainline. An artificial demand pattern is created to force demands above capacity in order to produce breakdown conditions on the freeway. The demands are gradually increased, sustained, and dropped over time. It is not possible to replicate a complete speed-flow graph without ramps. This test network was intended to represent the mainline freeway segment as specified in the Highway Capacity Manual, but two ramps had to be introduced in order to create the diversity in range of operations that would lead to a complete speed-flow graph.

CASE STUDY: US101, SAN MATEO, CA

Description

To demonstrate the usefulness of the proposed methodology and to provide results of comparison with current calibration procedures, a real-world freeway was simulated and calibrated using the described methodology. The case study network is a 5-mile 4-lane section on US101 Northbound in San Mateo, CA. A picture describing the extent of the simulation model and detector locations is provided in Figure 2. The data source is the California PeMS database (15). Data was collected over four detectors numbered 401199, 400935, 400007, and 400420; and from January 2, 2007 to January 4, 2007 from 5AM to 10PM over each day. It was verified that all detectors were in good health and reporting throughout the data collection period.

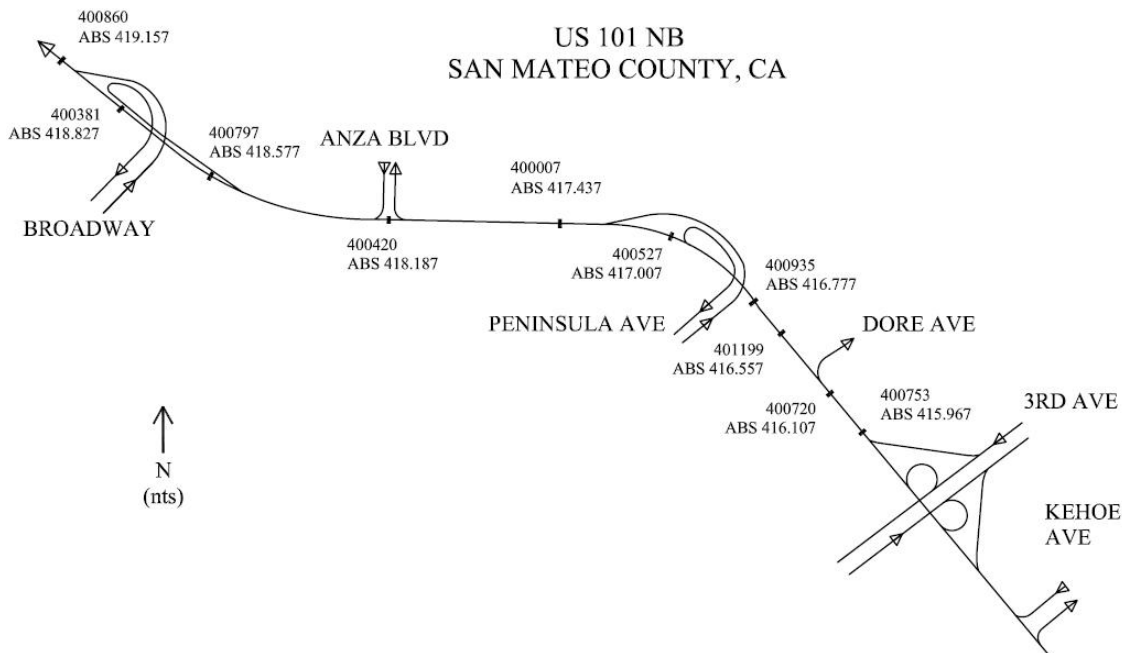


FIGURE 2 Extent of simulation for US101 NB, San Mateo, CA.

VISSIM Model

VISSIM 4.30 microsimulation software was used to develop and test the calibration procedure. VISSIM is based on a psycho-physical car-following model and uses perception thresholds to model drivers (14, 15). The model was coded for the extent provided in Figure 2 and detectors were placed at exactly the same position as reported by California PeMS database (21). Speeds and flows are aggregated and averaged over lanes over a 5 minute interval. This aggregation over time and space follows the procedures published by PeMS (21). In addition, a test network similar to one illustrated in an earlier section was developed to test the applicability of test networks to assist in calibration of simulation models.

VISSIM Driver Behavior Calibration Parameters

The following five calibration parameters were used in the calibration procedure.

1. CC1: The headway time (in seconds) that the driver wants to keep between vehicles.
2. CC2: Following variation - controls longitudinal oscillation in the car-following process.
3. CC3: Threshold for entering car-following - controls the start of the deceleration process, i.e. when a driver recognizes a preceding slower vehicle.
4. CC4: Following threshold - controls the speed differences during closing in following process.
5. CC5: Following threshold - controls the speed differences during opening in following process.

For a more detailed explanation of VISSIM microsimulation and the calibration parameters, please refer to the VISSIM 4.30 user manual (16).

Optimization Algorithm

There are many optimization algorithms that can be used in the calibration of microsimulation. For the past few years, Evolutionary Algorithms (EA) has been successfully applied in traffic microsimulation

calibration ((4), (17), and (18)). EA is one of the many algorithms based on principles of natural selection and can be considered as an extension to a simple or a canonical genetic algorithm over types of representation, crossover, mutation, and selection. EA also saves the elite individual with the best fitness value over generations. An EA tool in MATLAB, a scientific programming tool, was used for calibrating the simulation models. As is customary in publications involving EA, a pseudo-code is presented below:

Pseudo-Code for the Evolutionary Algorithm

```

BEGIN
  INITIALIZE population with random candidate solutions
  EVALUATE individual candidates
  REPEAT UNTIL (TERMINATION CONDITION is satisfied) DO
    SELECT parents
    RECOMBINE pairs of parents
    MUTATE the resulting offspring
    CHECK if candidates are already evaluated
    EVALUATE candidates not previously evaluated
    STORE fitness values
    SAVE elite individual
    SELECT elite individual and remaining individuals for the next generation
  END
END

```

EA performs the optimization process based on multiple evaluations of the objective function. The candidates for the next generation are selected based on fitness values. However, the elite individual (best fitness seen yet) is sent to the next generation without mutation. The EA can be implemented using different representations like real-number, binary, gray-coded, etc. The EA was tested for each of the representations, and real-number representation performed slightly better than binary and gray-coded representations. The recombination, mutation, and selection were chosen to improve diversity, which is paramount to achieving a global optimum. Proportional scaling of fitness values and roulette wheel method was employed for selection. Gaussian methodology was used for mutation. It is possible to choose more than one elite individual to send to the next generation, but increasing the number of elite individuals usually results in a premature convergence due to decreased diversity. Each simulation model was run for 3 simulation-hours and for five different random seeds. The evolutionary algorithm used 10 members per population and 5 runs per member. Since there is possibility that some of the individuals might be repeated in future generations, the fitness values for individuals were stored in a database to reduce computation times. The total run times varied for the evolutionary algorithms ranged from 12 to 30 hours based on the objective function.

RESULTS

In this section the results from three different applications of the methodology are presented.

1. Calibration of test network to the objective functions
2. Calibration of US101NB to the objective functions
3. Application of test-network-calibrated parameter values to US101NB

The first application is on the test network shown in Figure 3 and the second and third application on the US101 freeway network shown in Figure 4. For each scenario, 5 runs were performed, each run being 3 simulation-hours. Five minute speed and flow data were collected from the mainline detectors. The data from multiple runs were aggregated and the speed-flow graphs were produced. The three objective functions consisted of comparisons between the field and simulated data for:

- a. Maximum five minute flows (Maximum Flow)
- b. Maximum five minute flows sustained over 15 minutes (Sustained Flow)

c. Matching speed-flow graphs (Speed-Flow)

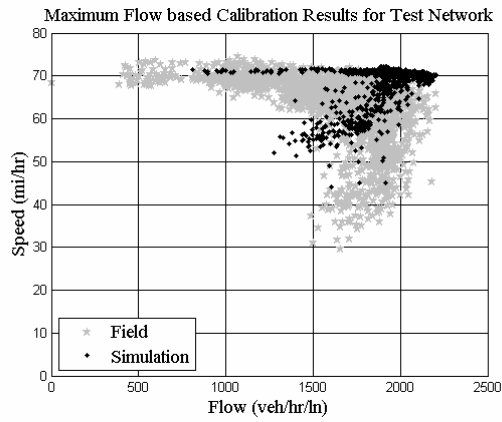
Test-Network

Figures 3.a-3.c show the results of the comparisons. The visual inspection of these three figures shows that the speed-flow objective resulted in the best match between field and simulated data. This is as expected since the objective function itself involves the minimization of non-overlapping speed-flow points. Figure 3.a shows that the maximum flow objective focuses solely on the highest flow values thus missing badly the congested regions of the speed-flow graph. Figure 3.b shows that while the sustained flow objective captures the congested region better than maximum flow, it does not produce the realistic scatter of data in the congested region as shown in Figure 3.c. Consequently, the matching of the shape of the speed-flow graph results in the most complete and realistic coverage of the speed-flow graph. Theoretically, this means that the simulation based on shape matching can better represent traffic during longer periods of time and not just the top five or fifteen minutes of the day. The practical implication is that the use of the new methodology would better capture the entirety of the peak period which typically lasts several hours in most metropolitan areas.

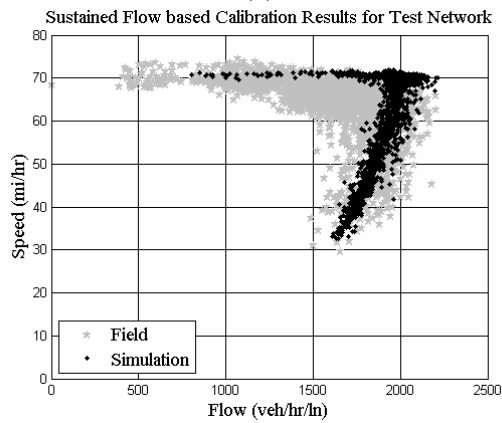
TABLE 1 Calibration Parameters for Test Network

Objective	CC1 (s)	CC2 (m)	CC3 (s)	CC4	CC5
Default Values	0.9	4	-8	-0.35	0.35
Speed-flow	1.28	8.11	-10.92	-0.45	1.06
Sustained flow	1.06	7.79	-5.66	-2.50	2.32
Maximum flow	0.83	12.02	-14.19	-1.42	2.31

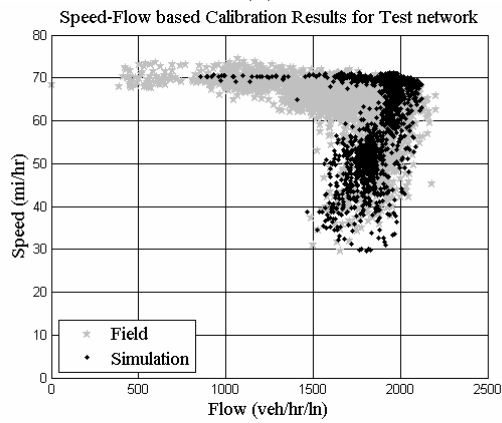
Table 1 shows the calibration values that resulted from the test network. The default values are provided in the first row to draw a comparison with the optimization suggested values. The CC1 column shows that speed-flow matching produces the longest CC1 value. This is expected since speed-flow matching involves the whole range of traffic conditions and not just the capacity or short headway conditions. CC2 and CC3 show similar trends in that the maximum flow produces the highest value while highest sustained flow produces the smallest value. Speed-flow is between those two values. For CC4 and CC5, the speed-flow results in a driver that is much more sensitive to speed differences between the leader and follower than capacity (rows 3 and 4). Table 1 shows that parameters calibrated using speed-flow graphs are significantly different from those calibrated using capacity.



(a)



(b)



(c)

FIGURE 3 Test network speed-flow graph comparisons for different objective functions.

US101 NB Network

Analogous to the test network cases, the same three objective functions were also applied to the US101 network. Figures 4.a-4.c show the results of the comparisons. Compared with the test network, the simulated US101 network produces a much more scattered pattern right before the pre-queue flow area. This might be explained due to existence of more varied traffic conditions for US101 NB than the test network. Once again the objective based on the matching of the speed-flow graphs produces the simulated speed-flow graph that matches the field data the most closely. Figure 4.a shows that maximum flow objective results in a speed-flow graph that is shifted to the left, so flows in the congested region are underestimated significantly. On the other extreme, the sustained flow objective results (Figure 4.b) in a graph shifted to the right so flows are overestimated. It is only the third objective function that produces the closest match for all traffic regions of the speed-flow graph (Figure 4.c).

Table 2. Calibration Parameters for US101 NB

Objective	CC1 (s)	CC2 (m)	CC3 (s)	CC4	CC5
Default Values	0.9	4	-8	-0.35	0.35
Speed-flow	1.09	10.59	-7.91	-2.50	0.64
Sustained flow	1.12	2.98	-5.5	-2.59	2.46
Maximum flow	0.83	12.12	-7.7	-2.20	1.17

Table 2 shows the calibration values that resulted from the simulated US101 network. The first column, CC1, shows that maximum flow produces the smallest value of headway which means overly aggressive driving. The second column, CC2, shows that sustained flow produces fairly insensitive behavior to longitudinal oscillation that is unrealistic. The third column, CC3, shows that sustained flow produces a smaller value for the car-following threshold. The other interesting observation is that CC3 values suggested by both test network and US101 were close to the default values suggested by VISSIM.

CC4 and CC5 are speed thresholds in following for closing and opening process. For example, in VISSIM, when a car is in following condition the driver tries to hold the acceleration values to a minimum. The driver reacts when one of the following speed thresholds is broken. In addition, CC2 also control the oscillation and also results in driver reaction during following process. Therefore, in a closing condition, if speed differences exceed absolute value of CC4, the driver reacts by braking. Analogously, if CC5 is broken, the driver reacts in an opening condition by accelerating. Intuitively speaking, CC4 and CC5 should exhibit an asymmetrical behavior since drivers are more sensitive when closing than when opening. The speed-flow objective values for CC4/CC5 were not in compliance with this and the values suggested by speed-flow objective are very different from the default values in VISSIM. However, the results of the test network are in compliance with this effect.

In order to truly understand the reason behind non-compliance of CC4 and CC5 values, vehicle trajectory data from Next Generation Simulation (NGSIM) (19) was plotted as shown in Figure 5. The interesting observation is related to US101 NB calibrated CC2, CC4, and CC5 values. The values suggested by the simulation model are quite similar to the values observed from US101 NGSIM vehicle trajectory data. A sample vehicle trajectory data represented using relative velocity of and relative distance is shown in Figure 5. The following thresholds suggested by speed-flow objective in Table 2 have been overlaid over the vehicle trajectory obtained from US101 NGSIM data. The graph shows the thresholds suggested are in good confirmation with real-world data. Since the thresholds defined by CC4 and CC5 are not speed dependent, the values are average values used for all speed levels. The field observation based on NGSIM vehicle trajectory data is not in compliance with intuitive observation of asymmetry in CC4 and CC5. Throughout all the parameters, the values derived from shape matching results in the most reasonable values according to traffic flow theory.

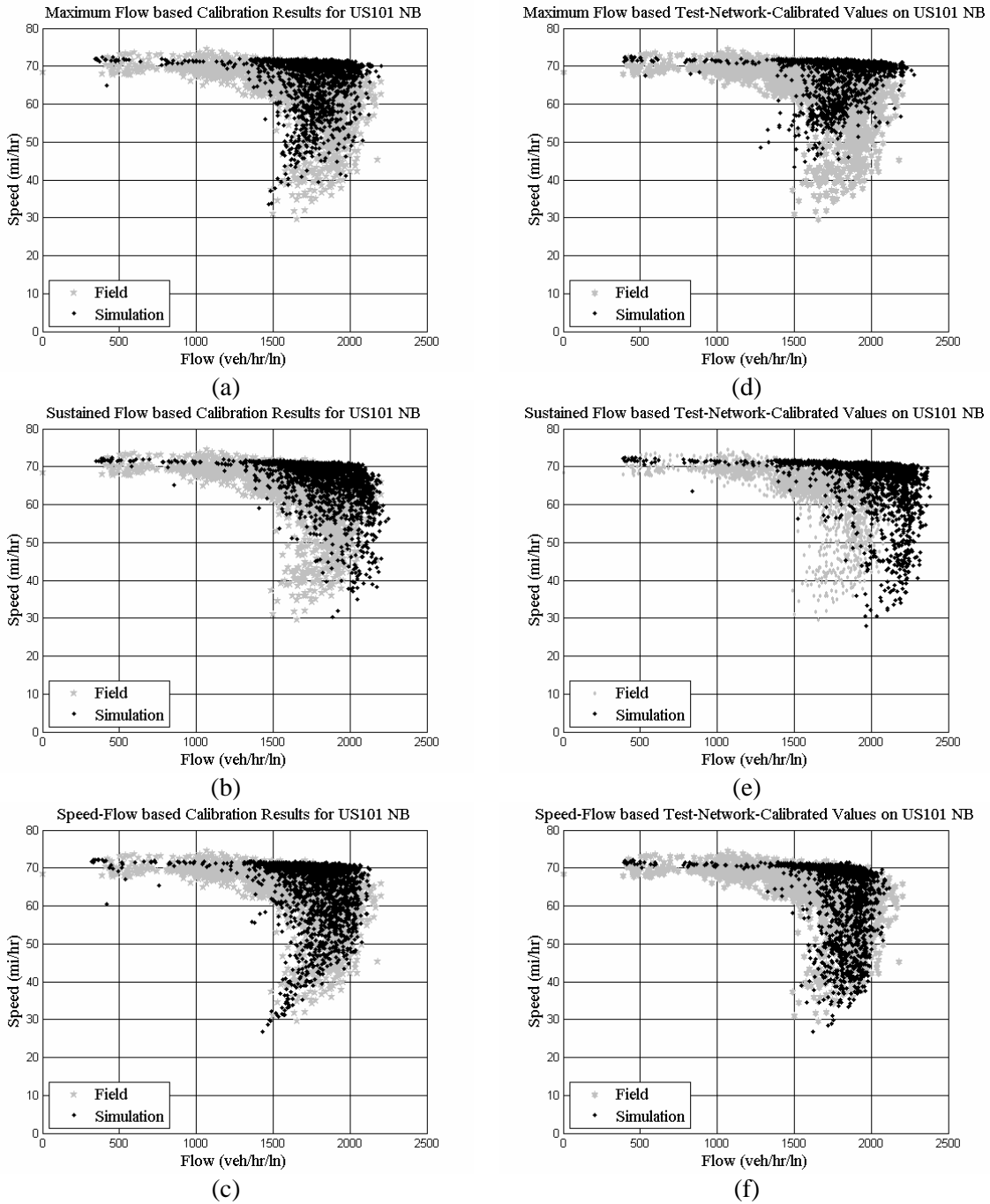


FIGURE 4 Speed-flow graph comparisons for US101 NB using different objective functions.

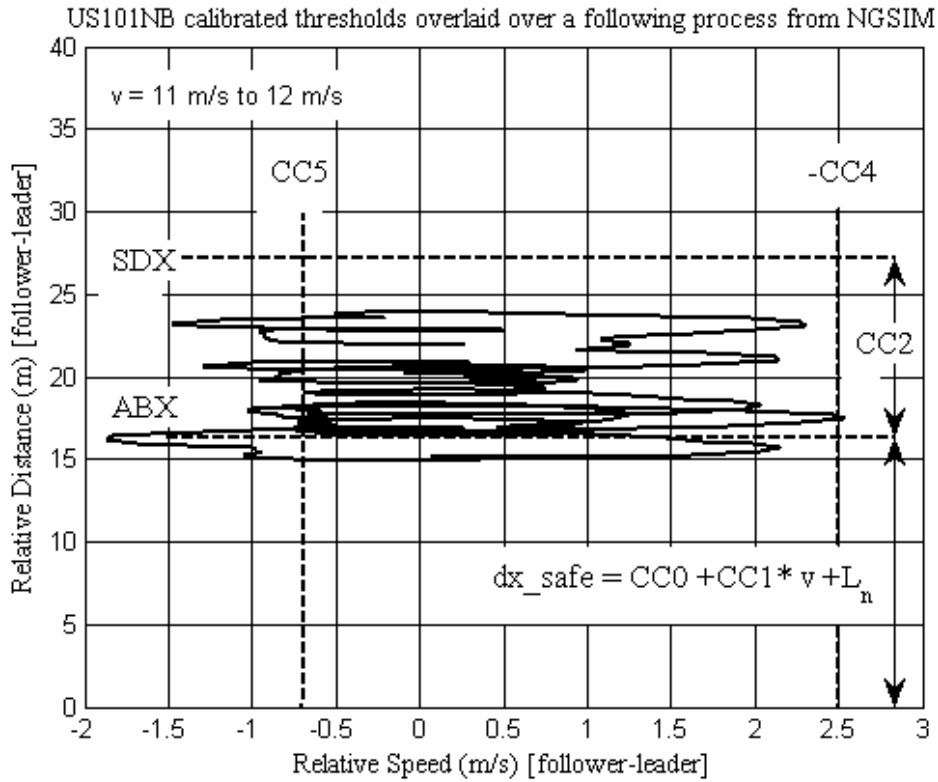


FIGURE 5 US101NB calibrated thresholds overlaid over a vehicle trajectory from NGSIM.

Test-Calibrated-Values Applied to US101 NB

In order to evaluate the applicability of using test network to calibrate an actual network, the test-network-calibrated values for each of the objective functions is fed into the US101 NB simulation model. The results of such a comparison are provided in Figures 4.d-4.f. Table 3 shows the speed-flow objective evaluations on each of the graphs in Figure 4. Speed-flow objective give a sense of dissimilarity of graphs. The lower the value of objective the better the match is between the graphs. The comparison amongst these values is fair, because the speed-flow measurements are made over the same simulation model (US101 NB) resulting in equal number of observations. The comparison amongst graphs produced from test network and US101 NB is not fair, because the number of observations on test network is not equal to US101 NB. Figures 4.c and 4.f are fairly similar to each other. The speed-flow objective evaluation for these graphs (Table 3) shows a 10% variation in objective function value for speed-flow based calibration. A much higher variation is observed for the other objective functions. However, the graph achieved using test-network-calibrated values for speed-flow objective is quite comparable to the ones achieved using US101 NB. In addition, the test network can take advantage of time again when applied to large scale simulation models.

TABLE 3 Speed-Flow Objective Evaluations for US101 NB Speed-Flow Graphs

Objective	Speed-Flow Objective Fitness Values	
	Calibration using US101 NB	Test-Network-Calibrated values on US101 NB
Speed-flow	193	210
Sustained flow	244	317
Maximum flow	237	293

CONCLUSIONS

A new methodology for calibrating microsimulation was presented. This new methodology introduced the use of speed-flow graphs as a calibration objective, defined a fitness function for point sets, and included an automated technique for optimization based on Evolutionary Algorithm. Encouraging results were obtained from the application on the US101 freeway in California. The results from speed-flow objective function have been shown to perform better than the objective function based on maximum 5-min. flow and maximum 5-min. flow sustained for 15 minutes. The calibration parameter values from the speed-flow calibration are shown to perform well in all three regions of the speed-flow graph: free-flow, congested, and discharge. The speed-flow objective calibrated parameter values resulted in a scatter in speed-flow graphs similar to the field graphs. This accounts for the stochastic nature of speed and flow observations on the field. The results suggested by the Evolutionary Algorithm based on speed-flow objective are plausible and sometimes even close to default values. The evolutionary algorithm suggested calibration parameter values resulted in speed-flow graphs similar to the one noticed in the field. It is important to note that the evolutionary algorithm could have suggested physically unreasonable calibration parameter values, if the degree of freedom was too high. The objective function can be expected to perform similarly even if a different search and optimization method was employed. But the comparative efficiencies of the search and optimization methods are beyond the scope of the paper. It can also be seen that test networks can be employed to assist in calibration of parameter values when the simulation networks are large.

Much of this study was concentrated on demonstrating the applicability of matching speed-flow graphs for microsimulation calibration. The study was implemented using an evolutionary algorithm. It might be worthwhile to compare other search and optimization methods to the evolutionary algorithm. In addition, the algorithm can be made more intelligent to reduce the number of simulation runs and improve run times. The study also concentrated only on a few driver behavior parameters, studying the effect of other driver behavior parameters like the probability of lack of attention is useful for better understanding the simulation model.

ACKNOWLEDGMENT

One of the authors (S.M.) would like to thank James Rice for his invaluable assistance all through the project.

REFERENCES

1. Dowling, R., A. Skabardonis, J. Halkias, G. McHale, and G. Zammit. Guidelines for Calibration of Microsimulation Models: Framework and Applications. In *Transportation Research Record: Journal of the Transportation Research Board, No. 1876*, TRB, National Research Council, Washington, D.C., 2004, pp. 1–9.
2. Hourdakis, J., P. G. Michalopoulos, and J. Kottommannil. Practical Procedure for Calibrating Microscopic Traffic Simulation Models. In *Transportation Research Record: Journal of the Transportation Research Board, No. 1852*, TRB, National Research Council, Washington, D.C., 2003, pp. 130–139.
3. Toledo, T. M. E. Ben-Akiva, D. Darda, M. Jha, and H. N. Koutsopoulos. Calibration of Microscopic Traffic Simulation Models with Aggregate Data. In *Transportation Research Record: Journal of the Transportation Research Board, No. 1876*, TRB, National Research Council, Washington, D.C., 2004, pp. 10–19.
4. Schultz, G. G., and L. R. Rilett. Analysis of Distribution and Calibration of Car-Following Sensitivity Parameters in Microscopic Traffic Simulation Models. In *Transportation Research Record: Journal of the Transportation Research Board, No. 1876*, TRB, National Research Council, Washington, D.C., 2004, pp. 41–51.
5. Gomes, G., A. May, and R. Horowitz. Congested Freeway Microsimulation Model Using VISSIM. In *Transportation Research Record: Journal of the Transportation Research Board, No. 1876*, TRB, National Research Council, Washington, D.C., 2004, pp. 71–81.
6. *Highway Capacity Manual*. TRB, National research Council, Washington, D. C., 2000
7. Brilon, W., J. Geistefeldt, and H. Zurlinden. Implementing the Concept of Reliability for Highway Capacity Analysis. Presented at 87th Annual Meeting of the Transportation Research Board, Washington, D.C., 2007.
8. Banks, J. H. The Two-Capacity Phenomenon: Some Theoretical Issues. In *Transportation Research Record: Journal of the transportation Research Board, No. 1320*, TRB. National Research Council, Washington D. C., 1991. pp. 234-241.
9. Wiedemann, R. *Simulation des Straßenverkehrsflusses* (in German). Schtiffenreihe des Instituts fur Verkehrswesen der Universitat Karlsruhe, Heft 8, Germany, 1974.
10. Wiedemann, R. Modelling of RTI-Elements on Multi-Lane Roads. In *Advanced Telematics in Road Transport*, Vol. II, Elsevier, Amsterdam, Holland, 1991, pp. 1001–1019.
11. Fellendorf, M. and P. Vortisch. Validation of the Microscopic Traffic Flow Model VISSIM in Different Real-World Situations. Presented at 80th Annual Meeting of the Transportation Research Board, Washington, D.C., 2001.
12. Ngoduy, D., S. P. Hoogendoorn, and H. J. V. Zuylen. Comparison of Numerical Schemes for Macroscopic Traffic Flow Models. In *Transportation Research Record: Journal of the Transportation Research Board, No. 1876*, TRB, National Research Council, Washington, D.C., 2004, pp. 52–61.
13. May, A. D. *Traffic Flow Fundamentals*, Prentice-Hall Inc., New Jersey, 1990.

14. Pekalska, E., and R. P. W. Duin. *The Dissimilarity Representation for Pattern Recognition*. World Scientific Publishing Co. Pte. Ltd., Singapore, 2005.
15. PeMS. *Freeway Performance Measurement System*. California Partners for Advanced Transit and Highways. University of California Berkeley and California Department of Transportation. <http://PeMS.EECS.Berkeley.EDU>. Accessed June, 2007.
16. PTV. *Vissim User Manual—V.4.30*. Planung Transport Verkehr AG, Karlsruhe, Germany, March 2007.
17. Ma, T., and B. Abdulhai. Genetic Algorithm-Based Optimization Approach and Generic Tool for Calibrating Traffic Microscopic Simulation Parameters. In *Transportation Research Record: Journal of the Transportation Research Board, No. 1800*, TRB, National Research Council, Washington, D.C., 2002, pp. 6–15.
18. Kim, K., and L. R. Rilett. Genetic-Algorithm-Based Approach for Calibrating Microscopic Simulation Models. *Proc., IEEE Intelligent Transportation Systems Conference*, IEEE, Oakland, Calif., 2001, pp. 698–704.
19. NGSIM. Home of the Next Generation Simulation Community. Federal Highway Administration. Washington D.C., <http://www.ngsim.fhwa.dot.gov/>. Accessed June, 2007.